

# The Marriage of Peripherally Metallated and Directly Linked Porphyrins: Bromidobis(phosphine)platinum(II) as a Cation-Stabilizing Substituent on Directly Linked and Fused Triply Linked Diporphyrins

Regan D. Hartnell,<sup>[a]</sup> Tomoki Yoneda,<sup>[b]</sup> Hirotaka Mori,<sup>[b]</sup> Atsuhiko Osuka,<sup>\*[b]</sup> and Dennis P. Arnold<sup>\*[a]</sup>

**Abstract:** A *meso*-bromidoplatiniobis(-triphenylphosphine)  $\eta^1$ -organometallic porphyrin monomer was prepared by the oxidative addition of *meso*-bromoZnDPP (DPP = dianion of 5,15-diphenylporphyrin) to a platinum(0) species. The *meso*-*meso* directly linked dimeric porphyrin (**5**) was prepared from this monomer by silver(I)-promoted oxidative coupling and planarized to give a triply linked dizinc(II) porphyrin dimer (**8**). Acidic demetallation of **8** afforded the bis(free base) **9**. Dimer **5** was demetallated then remetallated with nickel(II) to give the dinickel(II) analogue **10**, the X-ray crystal structure of which showed a twisted molecule with ruffled, orthogonal NiDPP rings,

terminated by square-planar *trans*-[Pt(PPh<sub>3</sub>)<sub>2</sub>Br] units. New compounds were fully characterized spectroscopically, and the fused diporphyrin exhibited a broad, low-energy, near-IR electronic absorption band near 1100 nm. Electrochemical measurements of this series indicate that the organometallic fragment is a strong electron donor towards the porphyrin ring. The triply linked organometallic diporphyrin has a substantially lowered first one-electron

oxidation potential (−0.35 V versus the ferrocene/ferrocenium couple (Fc/Fc<sup>+</sup>)) and a narrow HOMO–LUMO gap of 0.96 V. Solutions prepared for NMR spectroscopy slowly decompose with degradation of the signals, which is attributed to partial oxidation to the cation radical. This paramagnetic species can be reduced in situ by hydrazine to restore the NMR spectrum to its former appearance. The combined influence of the two [Pt(PPh<sub>3</sub>)<sub>2</sub>Br] electron-donating substituents is sufficient to make dimer **5** too aerobically unstable to allow further elaboration.

**Keywords:** electrochemistry • organometallic compounds • NMR spectroscopy • platinum • porphyrinoids

## Introduction

There has been considerable interest in the synthesis and properties of various types of organometallic porphyrins. These organometallic porphyrins have been investigated as model compounds for cytochrome P450 and coenzyme B<sub>12</sub> and to provide potential insight into several events of biological importance. Organometallic porphyrins have also been used for the activation of small molecules. Traditionally the “organometallic” nature of the molecule arises from

a metal–carbon bond between the metal bound in the central cavity of the porphyrin macrocycle with either an alkyl or aryl moiety of either  $\sigma$ - or  $\pi$ -bonding character.<sup>[1]</sup> Porphyrinoid macrocycles with modified cavities, such as inverted or “N-confused” porphyrins and azul- and carbaporphyrins,<sup>[2]</sup> as well as various expanded porphyrinoids,<sup>[3]</sup> have markedly extended the realm of traditional organometallic porphyrin chemistry. There are also several examples of porphyrinoid compounds covalently bound to organometallic fragments, such as metallocenes, or with one of the porphyrin pyrrolic rings or bonds participating in a  $\eta^5$ -pyrrolyl- $\pi$ -metal arrangement.<sup>[4]</sup>

Apart from the examples of organometallic porphyrins discussed above, there is another group of  $\eta^1$ -organometallic porphyrins that have been investigated recently in which the metal fragment is directly bonded to the periphery of the macrocycle. Recent reviews on these types of organometallic porphyrins have been published.<sup>[5]</sup> Arnold and co-workers first reported peripherally platinated and palladated porphyrins in 1998,<sup>[6]</sup> and later papers included several X-ray crystal structures of derivatives with different centrally coordinated metal ions,<sup>[7]</sup> as well as the only report of such complexes containing non-racemic chiral diphosphines.<sup>[8]</sup> More-

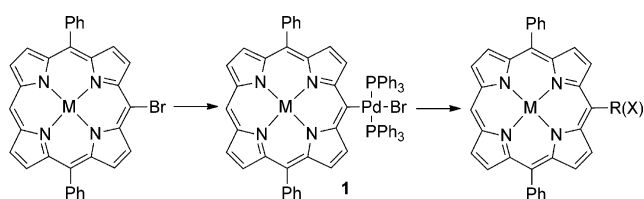
[a] Dr. R. D. Hartnell, Prof. D. P. Arnold  
School of Chemistry, Physics and Mechanical Engineering  
Queensland University of Technology  
G.P.O. Box 2434, Brisbane 4001 (Australia)  
Fax: (+61) 7-3138-2482  
E-mail: d.arnold@qut.edu.au

[b] T. Yoneda, H. Mori, Prof. A. Osuka  
Department of Chemistry, Graduate School of Science  
Kyoto University, Sakyo-ku, Kyoto, 606-8502 (Japan)  
Fax: (+81) 75-753-3970  
E-mail: osuka@kuchem.kyoto-u.ac.jp

Supporting information for this article is available on the WWW under <http://dx.doi.org/10.1002/asia.201300633>.

over, platinum(II) examples with chelating N-ligands and supramolecular multiporphyrin arrays<sup>[9]</sup> were also prepared. Osuka and co-workers more recently took advantage of their discoveries in selective  $\beta$ -arylation of porphyrins, to prepare and investigate palladium and platinum pincer complexes, in which the neutral supporting ligands were two  $\beta$ -2-pyridyl moieties.<sup>[10]</sup> Other examples include the  $\beta$ -palladio cyclometallated complexes reported by Matano et al.,<sup>[11]</sup> and N-confused porphyrin palladium(II) and platinum(II/IV) dinuclear complexes in which the exomacrocyclic metal ion is coordinated by the external nitrogen atom and an *ortho*-metallated *meso*-aryl ring.<sup>[12]</sup>

This type of transition-metal chemistry gives rise to compounds, such as **1**, which are key intermediates involved in palladium-catalyzed C–C or C–X coupling reactions of *meso*-haloporphyrins with various substrates (Scheme 1).<sup>[13]</sup>



Scheme 1.  $\eta^1$ -*meso*-Palladioporphyrins as intermediates in coupling reactions.

The initial step in these couplings is the oxidative addition of the *meso*-carbon–halogen bond to a zero-valent palladium species, usually a bis(phosphine) moiety. Indeed, our initial isolation of a *meso*-palladioporphyrin resulted from a failed catalytic reaction.<sup>[6]</sup> To expand our research in this field, we are investigating new porphyrinic systems in which to incorporate these organometallic fragments. Thus, we might be able to exploit both the electronic effects and supramolecular coordination possibilities of a robust organometallic fragment, and the remarkable optical and electronic properties of multi-porphyrin systems. As an initial foray into this area, we have prepared several new porphyrin dimers of the *meso*–*meso* directly linked class terminated uniquely by organoplatinum(II) fragments, and investigated their chemical, optical, and redox properties. By further oxidative coupling, triply linked (fused) diporphyrins were also prepared, and their chemistry revealed the profound electronic effects of the platinum(II) substituent.

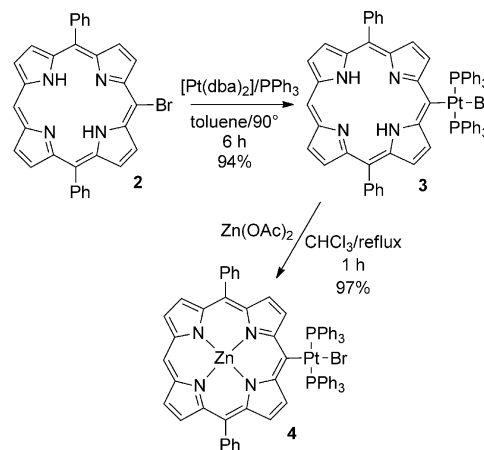
## Results and Discussion

### Synthesis and NMR Spectroscopic Characterization

Organometallic  $\eta^1$ -*meso*-platinio- and palladioporphyrins are readily prepared by the oxidative addition of a zero-valent metal precursor to a haloporphyrin.<sup>[6–9]</sup> The easiest way to prepare those compounds that utilize monophosphine supporting ligands (e.g., PPh<sub>3</sub> or PEt<sub>3</sub>) is by generating the desired zero-valent precursor in situ, so that it may

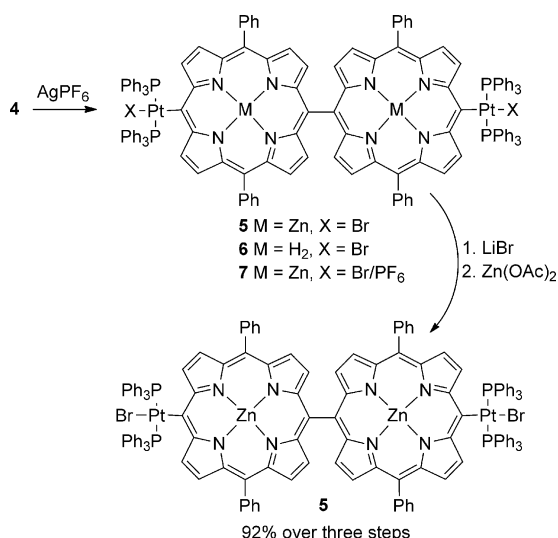
then immediately react with the desired haloporphyrin.<sup>[9]</sup> The newly formed zero-valent platinum species ([Pt(PPh<sub>3</sub>)<sub>3</sub>] or [Pt(PPh<sub>3</sub>)<sub>2</sub>(dba)]; dba = dibenzylideneacetone) undergoes an oxidative addition reaction with the haloporphyrin to form the organometallic *meso*-platinio porphyrin. The haloporphyrin is usually consumed within one hour, depending on the steric and electronic properties of the monophosphine (PPh<sub>3</sub> or PEt<sub>3</sub>), the haloporphyrin (whether Br or I), and the metal coordinated within the central cavity of the porphyrin macrocycle. The initial product that forms after oxidative insertion is the *cis* isomer, which isomerizes during heating for approximately five hours to give the more stable *trans* isomer.<sup>[7]</sup> These organoplatinum porphyrins are normally very air- and moisture-stable in solution for several weeks and indefinitely in the solid state, and may be purified by column chromatography on silica gel with no degradation, as long as solvents used in the chromatographic purification are de-acidified. Although free-base porphyrins may be used for the oxidative addition step, platinum coordination to the central cavity of the porphyrin does not occur. Other metal ions may then be coordinated within the central cavity of the porphyrin under typical metallation conditions, with no degradation of the organometallic fragment.<sup>[7b]</sup>

Herein, [Pt(dba)<sub>2</sub>] was treated with triphenylphosphine and **2** in degassed toluene at 90° for 6 h, resulting in excellent yields (>90%) of **3**. Then zinc(II) complex **4** was formed by heating free-base organometallic porphyrin **3** in chloroform at reflux with a saturated solution of zinc(II) acetate in methanol (Scheme 2). This metal insertion reac-



Scheme 2. Synthesis of ZnDPP[Pt(PPh<sub>3</sub>)<sub>2</sub>Br] **4**. DPP = dianion of 5,15-diphenylporphyrin.

tion was easily followed by TLC and UV-visible spectroscopy and was completed within one hour. Excess metal salt was removed by simply washing the product with water or by filtering the reaction mixture through a short plug of silica gel. Recrystallization of the residue and collection of the product gave an almost quantitative yield of zinc(II) **4**. The silver(I)-promoted dimerization of **4** was initially inves-



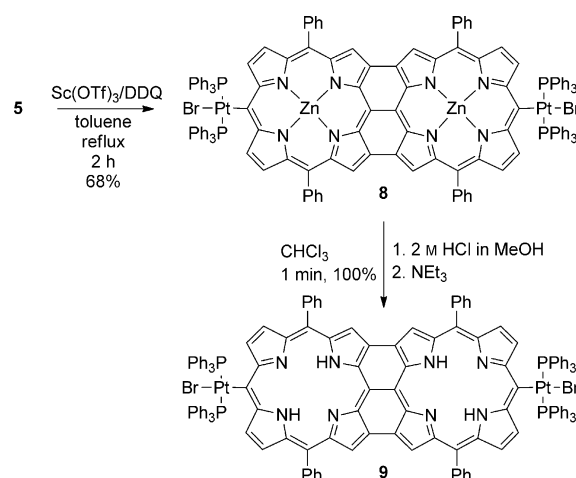
Scheme 3. Synthesis of *meso-meso*-linked diplatinated diporphyrin 5.

tigated by using the procedure of Osuka and co-workers (Scheme 3).<sup>[14–16]</sup> This utilizes half an equivalent of the one-electron oxidant ([AgPF<sub>6</sub>]) to maximize the populations of neutral and radical cationic porphyrin species because dimerization occurs by nucleophilic attack on the porphyrin radical cation by a neutral porphyrin. In the case of **4**, these reaction conditions were too mild and the reaction did not go to completion, even after prolonged reaction times. The low reactivity of the porphyrin radical cation is presumably due to the electron-donating effects of the organometallic fragment. However, when a fivefold excess of the oxidant was used, dimerization proceeded smoothly and the starting material was consumed within one hour.

The <sup>1</sup>H NMR spectrum of the crude product indicated a mixture of several products. The absence of porphyrin *meso*-proton signals showed that dimerization did indeed go to completion and the other compounds were various *meso-meso*-linked porphyrin dimers, as well as the desired dimer **5**. The presence of an NH resonance at  $\delta \approx -3$  ppm showed that one of the contaminants was the free-base analogue **6**. Separation of **5** and **6** was difficult by TLC, but the chromatograms did show the presence of a very polar spot, which was postulated to be the Br/PF<sub>6</sub> singly or doubly metathesized products, such as **7**, owing to bromide abstraction by excess silver(I). Instead of separating the desired dimer from various byproducts, a better method was to reverse the metathesis to re-form the desired dimer. This was readily achieved by heating the crude mixture with excess LiBr. Then all free-base species were re-metallated by the addition of excess zinc acetate as a saturated solution in methanol to the same reaction mixture at reflux. <sup>1</sup>H NMR spectroscopy analysis showed that indeed our ideas were correct because within one hour only the desired dizinc *meso-meso* linked dibromido dimer **5** was present. The reaction mixture was filtered through a short plug of silica gel to remove excess salts. After recrystallization, compound **5** was collected as dark olive-green crystals in 92% yield.

There are several significant changes to the <sup>1</sup>H NMR spectrum upon dimerization of **4**. First, the <sup>1</sup>H NMR spectrum of **5** displayed one set of porphyrin resonances, which indicated that the two halves of the dimer were equivalent. The absence of any porphyrin *meso*-proton resonances and the relative simplicity of the spectrum indicated that dimerization occurred exclusively at the *meso* positions and that no  $\beta$ -coupling reactions complicated the preparation of **5**. As expected, the  $\beta$ -hydrogen atoms nearest the direct *meso-meso* linkage underwent the biggest changes compared with monomeric **4**. In the spectrum of **5**, the signals of the  $\beta$ -hydrogen atoms nearest the *meso-meso* link were shifted upfield by  $\Delta\delta = 0.72$  and 0.92 ppm relative to those of **4**; this reflected the shielding effect of the second (orthogonal) porphyrin ring. The resonances of the distal  $\beta$ -hydrogen atoms were only slightly shifted after dimerization. These trends are now familiar in the literature.<sup>[15]</sup> The resonances for the phenyl hydrogen atoms of the phosphine ligands were shifted downfield by approximately 0.2 ppm in **5** relative to those of **4**. The <sup>31</sup>P NMR spectrum of **5** displays a singlet resonance at  $\delta = 23.3$  ppm for the four equivalent triphenylphosphine groups, which is flanked by <sup>195</sup>Pt satellites, with a Pt–P coupling constant of 2990 Hz; a typical value for *trans* phosphine groups in Pt<sup>II</sup> organometallics.<sup>[17]</sup>

Having obtained the directly linked species in high yield and purity, we attempted the oxidative double-ring closure/planarization of **5** by using the methodology of Osuka and Tsuda (Scheme 4).<sup>[17]</sup> Substrate **5** was heated at reflux with



Scheme 4. Synthesis of dizinc triply linked diporphyrin **8** and free-base **9**. DDQ = 2,3-dichloro-5,6-dicyano-1,4-benzoquinone.

DDQ and scandium(III) triflate in toluene for one hour. During this period, the reaction mixture changed from an olive-green color to bright blue-green, which indicated that a major change had occurred. After isolation and chromatography, the desired *meso-meso*, $\beta$ - $\beta$ , $\beta$ -triply linked dimer **8** was obtained in 68% yield. The <sup>1</sup>H NMR spectrum of **8** was relatively simple owing to the high symmetry of the molecule, but it was very clear that the desired planarization occurred. The distal  $\beta$  protons of **8** appeared as a pair of

broad doublets ( $J=4.4$  Hz) at  $\delta=8.72$  and 7.26 ppm. These resonances have been shifted significantly upfield by  $\Delta\delta=1.22$  and 1.24 ppm, respectively, relative to **5**, which demonstrates the large effects of planarization and the reduced aromatic ring current in the dimer.<sup>[16]</sup> The  $\beta$  protons next to the inter-ring bonds were represented by a broad singlet at  $\delta=7.19$  ppm. The resonances that arose from the phosphine phenyl groups were shifted slightly compared with **5**, especially the *m,p*-H resonances, which moved downfield by 0.3 ppm. Complete assignment of all proton resonances was facilitated by DQF-COSY and proton NOESY experiments. The <sup>31</sup>P NMR spectrum of **8** has a singlet at  $\delta=22.7$  ppm with a P–Pt coupling constant of 3016 Hz.

If the NMR sample was left as a solution overnight, the signal of the porphyrin dimer **8** degraded and no resonances from the  $\beta$ -H or phenyl groups could be detected. The only visible resonances were those of the phosphine groups, which were very broad (Figure 1, top). Isolation and recryst-

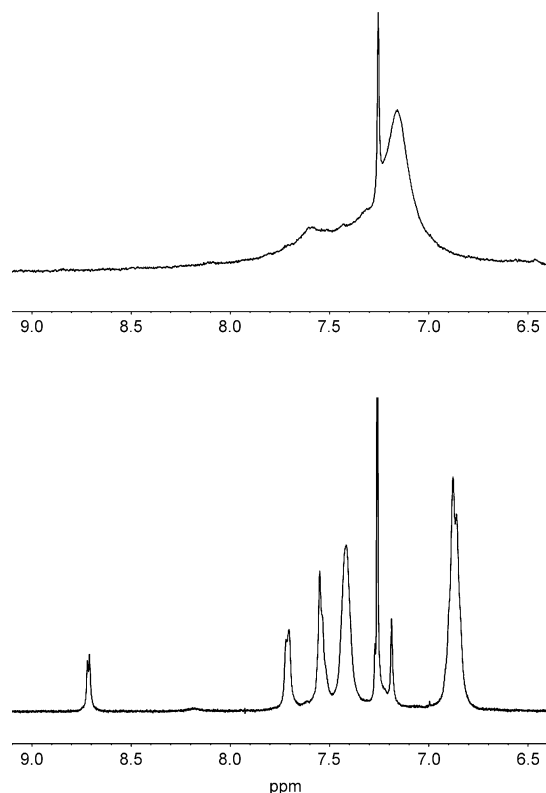


Figure 1. Downfield region of the <sup>1</sup>H NMR spectrum of **8** recorded in CDCl<sub>3</sub> before (top) and after (bottom) the addition of 80% hydrazine (20  $\mu$ L).

tallization of the sample, followed by preparation of a new solution for NMR spectroscopy, restored the spectrum to that previously seen. Similar behavior is known for zinc porphyrins that suffer from aggregation problems, although such spectra are usually improved by the addition of pyridine to act as an axial ligand and reduce intermolecular aggregation artifacts. The addition of [D<sub>5</sub>]pyridine to the

NMR sample of **8** did not cause any improvement to the degraded spectrum. Contemplation of these facts led us to believe that the porphyrin dimer was partially oxidized to the radical cation, producing a paramagnetic species and leading to the broadening of the NMR signals. Confirmation was provided by addition of hydrazine to the NMR sample to try to reduce the cation radical back to the neutral species. The signals of **8** were immediately restored, and the spectrum was then identical to that of the freshly prepared sample (Figure 1, bottom). Removal of hydrazine under high vacuum and preparation of a new sample for NMR spectroscopy revealed that the sample initially in the neutral state was slowly oxidized to the cation radical. Addition of hydrazine to this sample fully reduced the cation radical and restored normal NMR sensitivity.

Similar deterioration of the NMR signal was seen in <sup>31</sup>P NMR spectroscopy, which too was fully restored after the addition of hydrazine. To rule out aggregation phenomena as the cause of the problematic NMR spectroscopy, the central metal ions were removed (without cleaving the C–Pt bonds) from a small sample of **8** by treatment with 2 M HCl in methanol to produce free-base **9**. Addition of acid to **8** immediately gave a bright purple solution. Neutralization of this solution with excess triethylamine caused an immediate change, and the solution reverted to an intense green/blue color. The NMR spectrum of free-base **9** was similar to that of metallated **8**; this indicated that only demetallation of the macrocycle occurred, without cleavage of the platinum fragments. The signal arising from the free-base protons could not be definitively identified, and was possibly obscured by the broad H<sub>2</sub>O signal near  $\delta=1.5$  ppm; this is where this NH signal is found for similar compounds.<sup>[16]</sup> Similarly to the NMR behavior of **8**, the spectrum of **9** also dramatically improved after the addition of hydrazine. This suggests that a small population of both **8** and **9** prefers to exist as the radical cation in solution and is easily reduced to the neutral species by treatment with hydrazine. The ESI mass spectrum of **8** (Figure 2) displayed a strong cluster at  $m/z$  2643.26, which corresponded very well with the predicted isotope pattern (calculated for  $[M+H]^+$ :  $m/z$  2643.27) for the assigned structure of **8**.

### X-ray Crystal Structure Determination

Unfortunately the sensitivity of dimers **8** and **9** to light and air precluded us from obtaining single crystals suitable for X-ray analysis. Because nickel(II) porphyrins are more difficult to oxidize than the zinc(II) complexes, the directly linked dizinc dimer **5** was demetallated to **6** then remetallated with nickel(II) bis(acetylacetonate) to yield dimer **10** (Scheme 5). Single crystals of this analogue were grown from a solution in dichloromethane/pentane, and the molecular structure is shown in Figure 3. This is the first crystal structure of a *meso-meso*-directly linked nickel(II) diporphyrin, although other similar compounds, namely, copper(II)<sup>[18]</sup> and free-base diporphyrins,<sup>[19]</sup> zinc(II) triporphyrins,<sup>[20]</sup> and more complex arrays<sup>[21]</sup> have been reported.

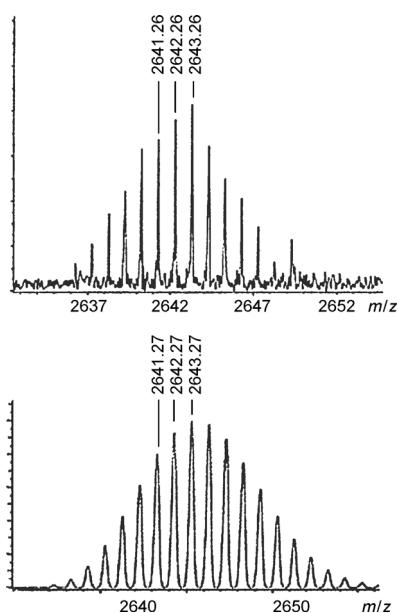
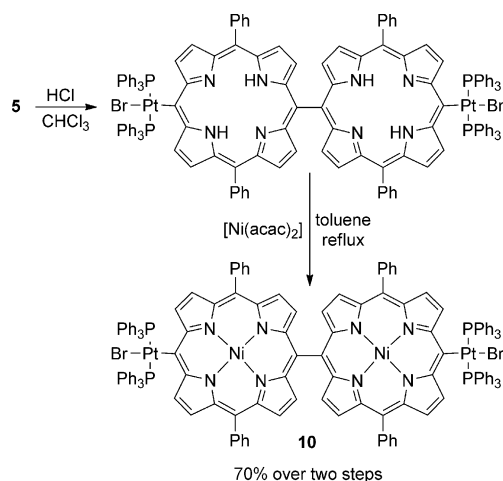


Figure 2. Experimental (top) and calculated isotopic distribution pattern (bottom) of  $[M+H]^+$  for **8**.



Scheme 5. Synthesis of dinickel *meso-meso*-linked diplatinated diporphyrin **10**. acac = acetylacetonate.

The two macrocycles in the molecule of **10** are strongly ruffled, which is often found for *meso*-tetrasubstituted nickel(II) porphyrins,<sup>[22]</sup> including other dimers with 5,15- or 5,10-diaryl substituents.<sup>[13g,23]</sup> Typically for a directly linked diporphyrin, the macrocycles are almost orthogonal. These two demands result in a curved, twisted overall geometry; the two views shown in Figure 3a and b make this clear. The single bond between the porphyrins is 1.492(15) Å long, which is the same as those recorded previously for structures of analogous di- and triporphyrins. The coordination planes of the platinum(II) units are also near-orthogonal to their attached macrocycles, but the two *meso*-C-Pt-Br vectors are not parallel. The Pt-C bond lengths are equal, within experimental error, at 2.026(14) and 1.987(14) Å. The coordination geometries at the platinum(II) centers are almost

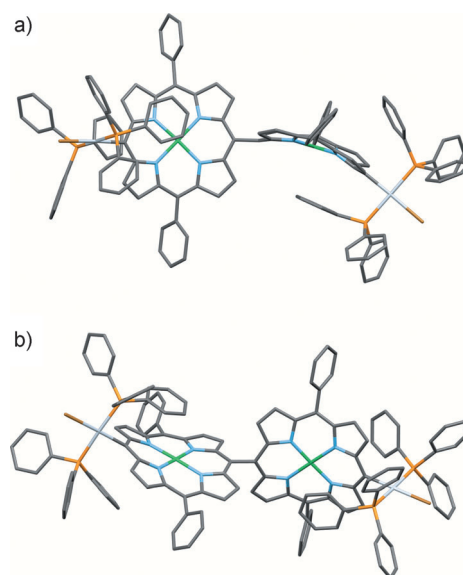


Figure 3. The X-ray crystal structure of **10**: a) the coordination geometry about the Pt<sup>II</sup> centers, the orthogonality of the porphyrin rings, the ruffling of the Ni<sup>II</sup> porphyrin units, and the disposition of two phenyl groups of the triphenylphosphine ligands above and below the planes of the porphyrin rings; and b) the orientations of the {Pt(PPh<sub>3</sub>)<sub>2</sub>Br} substituents. Hydrogen atoms and solvent molecules omitted for clarity.

square planar, with a very minor tetrahedral distortion. In our previous reports on the crystal structures of *meso*-metalloporphyrins with phenylphosphine ligands, we noted that one of the three rings of each phosphine lay over the macrocycle,<sup>[7]</sup> and this is emphasized in Figure 3a.

So far, we have been unable to characterize the triply linked systems crystallographically, but the NMR and other spectroscopic data confirm the integrity of the terminal [Pt-(PPh<sub>3</sub>)<sub>2</sub>Br] units, and the fusion of the porphyrins.

### Electronic Absorption Spectra

The electronic absorption spectra of dimeric **5** and **8** are compared in Figure 4. Complex **4** displays a normal electronic spectrum for a zinc porphyrin: a sharp Soret band at  $\lambda = 430$  nm and weak Q bands at  $\lambda = 555$  and 599 nm. Typical

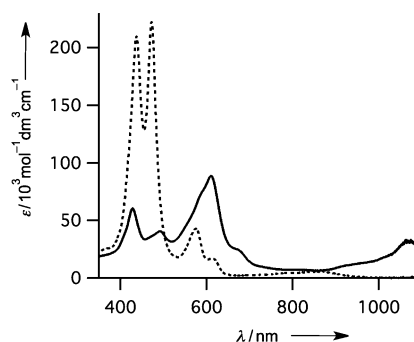


Figure 4. The electronic absorption spectra of *meso-meso* linked **5** (dashed) and triply linked **8** (solid).

changes are seen after dimerization through a *meso-meso* linkage. The most dramatic of these is the splitting of the Soret band in **5**, with peaks at  $\lambda = 437$  and  $470$  nm of similar intensity. Understandably there is a reduction in the extinction coefficient of these two peaks, compared with monomeric **4**. The characteristic appearance of the Soret bands indicates that the planes of the two porphyrins are essentially perpendicular to each other, that is, a  $D_2$  twisted conformation.<sup>[14–16]</sup> Thus, there is a strong excited-state interporphyrin interaction, but no conjugation in the ground state. The Q bands of **5** are also redshifted by 20 nm. After oxidative double ring-closure, the absorbance spectrum of **8** is strongly perturbed and indicative of a totally conjugated bisporphyrin system.<sup>[16,17]</sup> There is now a large splitting of the bands (labeled I and II), formerly attributable to the Soret bands in **4** and **5**, and the lowest energy band (III) extends well into the near-IR region beyond  $\lambda = 1100$  nm. In addition, the {PtL<sub>2</sub>Br} substituents induce a further redshift because the lowest-energy band for the Ni<sub>2</sub> analogue with aryl groups in the terminal 15,15'-positions has a maximum at  $\lambda = 933$  nm.<sup>[16]</sup> Bands I and II have been assigned to Soret-like transitions along the two axes of the molecule (short and long, respectively). The high intensity of band III, compared with simple monomeric porphyrins, arises from the loss of degeneracy in the unoccupied levels, and the redshift to the strong splitting of the monomer occupied and unoccupied frontier orbitals, which narrows the HOMO–LUMO gap of the dimer. The lowering of the energy of this transition by the organometallic substituents is a result of their electron-donating tendency, apparently raising the energy of the HOMO further. This is consistent with the voltammetry results described below.

The absorption spectra of zinc(II) **8** and free-base **9** did not show any substantial changes after the addition of hydrazine. This presumably indicates that there is only a small population of the radical cation in solution and it is not detectable by either UV-visible or near-IR spectroscopy. In the case of **8**, there was a slight redshift of all peaks after the addition of hydrazine, which may be interpreted as a manifestation of the axial coordination of hydrazine to the zinc(II) centers.

The emission properties of this series have not been investigated because monomeric free-base and zinc(II) porphyrins peripherally metallated with [Pt(PPh<sub>3</sub>)<sub>2</sub>Br] have fluorescence quantum yields about 1000-fold less than their unsubstituted analogues.<sup>[24]</sup> We expect similar measurements for the present series would also be unrewarding, although understanding the effects of these heavy-metal substituents on the emission properties of porphyrins is a future target.

### Electrochemical Investigations

Initially we wished to investigate the effect of the organometallic fragment on the redox properties of the porphyrin ring. Cyclic voltammetry measurements were carried out on ZnDPP (as a reference compound) and platinum complexes **4**, **5**, and **8**. Experiments were carried out in CH<sub>2</sub>Cl<sub>2</sub> contain-

ing 0.5 M Bu<sub>4</sub>NPF<sub>6</sub> as the supporting electrolyte, with a standard three-electrode cell under an atmosphere of nitrogen. Electrochemical measurements of ZnDPP were carried out on a saturated solution, owing to poor solubility of ZnDPP in the electrolyte-rich solvent, which gave rise to relatively high background current. Interestingly for platinum complexes **4**, **5**, and **8**, the presence of the electrolyte in the solvent seemed to improve the solubility of the substrates, so the measurements were performed on solutions with a porphyrin concentration of about 10<sup>-3</sup> M. Accurate measurements of the second reductive waves could not be made on **4** and **5**, and the reductions of ZnDPP were irreversible and poorly characterized. The derived data are shown in Table 1.

Table 1. Cyclic voltammetry data for reference monomer ZnDPP, monomer platinum complex **4**, and dimers **5** and **8** in Bu<sub>4</sub>NPF<sub>6</sub>/CH<sub>2</sub>Cl<sub>2</sub> versus the ferrocene/ferrocenium couple (Fc/Fc<sup>+</sup>) at 0.00 V.

	$E_{\text{red2}}^0$ [V]	$E_{\text{red1}}^0$ [V]	$E_{\text{ox1}}^0$ [V]	$E_{\text{ox2}}^0$ [V]	$\Delta E(\text{ox})$ [mV] <sup>[a]</sup>	$\Delta E(\text{gap})$ [V] <sup>[b]</sup>
ZnDPP	–	–	+0.30	+0.75	–	–
<b>4</b>	–	–1.73	+0.20	+0.55	–	1.93
<b>5</b>	–	–1.94	+0.15	+0.26	110	2.09
<b>8</b>	–1.6	–1.31	–0.35	+0.07	420	0.96

[a] The voltammetric gap between the first and second one-electron (per porphyrin unit) oxidations. [b] The electrochemical HOMO–LUMO gap ( $\Delta E(\text{gap}) = E_{\text{ox1}}^0 - E_{\text{red1}}^0$ ).

The platinum-containing species showed reproducible and reversible first and second oxidation waves in all cases. The first oxidation potentials of ZnDPP and **4**, +0.30 and +0.20 V (vs. Fc/Fc<sup>+</sup>), respectively, clearly demonstrate the cation-stabilizing effect of the platinum(II) fragment. The cathodic shift of 100 mV supports the premise that the *meso*-bonded {Pt(PPh<sub>3</sub>)<sub>2</sub>Br} fragment is an electron donor. However, this cathodic shift is somewhat smaller than that reported for similar free-base and nickel(II) *meso*-platinio-porphyrins, which exhibited a larger cathodic shift of approximately 300 mV.<sup>[7b]</sup> A second reversible oxidation of **4** was seen at +0.55 V ( $\Delta E_{\text{ox}} = 350$  mV). The first reduction potential of **4** is at –1.73 V, which translates to an electrochemical HOMO–LUMO gap of 1.93 V. Singly linked dimer **5** displayed two closely spaced one-electron redox waves, typical for other *meso-meso* linked dimers,<sup>[16]</sup> owing to the removal of one electron from each of the orthogonal porphyrin macrocycles. The first and second oxidation potentials for **5** are +0.15 and +0.26 V ( $\Delta E = \text{ca. } 110$  mV), respectively, which compare well with that of the *meso-meso* analogue that lacks the organometallic fragments, which displays splitting of the first two oxidation potentials of 130 mV.<sup>[16]</sup> Unfortunately, direct comparisons of actual half-wave potentials are not possible owing to different solvents and electrolyte concentrations used for the electrochemical measurements of our compounds and those in the literature, but the trends are consistent. Arnold and co-workers discussed the frequent over-interpretation of such “mixed-valence” splittings in diporphyrins as being directly indicative of the degree of inter-porphyrin conjugation.<sup>[25]</sup> Because

values of about 100 mV are also seen in indisputably strongly conjugated dimers, such as bis(porphyrinyl)butadiynes, such conclusions are invalid when comparing different linkage types and planar conjugated dimers with orthogonal dimers that are not conjugated.

Comparison of the first oxidation potentials between **4** and **5**, +0.20 and +0.15 V respectively, confirms that there is only slight elevation of the HOMO after dimerization. The first reduction potential of **5** occurs at -1.94 V, with a voltammetric HOMO-LUMO gap of 2.09 V, which is actually larger than that of **4**, demonstrating again the lack of electronic interaction between the rings in the ground state. Planarization of **5** through oxidative double ring closure results in several interesting electrochemical changes. The full cyclic voltammogram of **8**, including first and second reduction and oxidation potentials, was measured and was sufficiently well defined to reveal some interesting electrochemical properties of this compound (Figure 5).

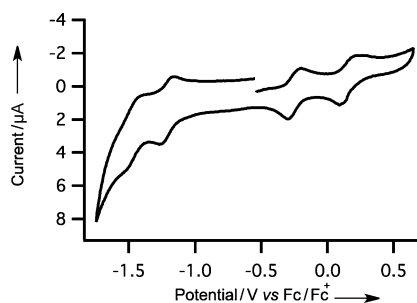


Figure 5. Cyclic voltammogram (100 mV s<sup>-1</sup>) for dimer **8** in Bu<sub>4</sub>NPF<sub>6</sub>/CH<sub>2</sub>Cl<sub>2</sub>, versus Fc/Fc<sup>+</sup> at 0.00 V.

The first of these is the dramatic lowering of the first oxidation potential for **8** ( $E_{\text{ox1}}^0 = -0.35$  V) by approximately 500 mV when compared with **4** and **5**. The second reversible oxidation occurs at +0.07 V, with  $\Delta E_{\text{ox}} = 420$  mV. This is very similar to that found for the Ni<sub>2</sub> dimer reported by Osuka and co-workers (410 mV CHCl<sub>3</sub>).<sup>[16]</sup> Diederich and co-workers reported voltammetric data for a series of directly linked and triply linked dizinc diporphyrins with 15,15'-aryl substituents that were subsequently conjugated to fullerenes.<sup>[26]</sup> In their case, however, the "mixed-valence" oxidative splitting was only 290 mV, which was very similar to that for the dizinc diporphyrin reported by Osuka and co-workers (250 mV in CHCl<sub>3</sub>).<sup>[16]</sup> The significance of the considerably smaller gap for zinc(II) is presently unclear, and spectroelectrochemical studies are required to determine this.

The first and second reduction potentials (-1.31 and -1.57 V, respectively,  $\Delta E_{\text{red}} = 260$  mV) were also reversible, although the waves were near the solvent limit under our conditions. From these half-wave potentials, planarization to form **8** results in substantial raising of the HOMO and lowering of the LUMO, to give a HOMO-LUMO gap of only 0.96 V, which is less than half of that for dimer **5**. This HOMO-LUMO gap is compatible with the redshifted near-

IR band near  $\lambda = 1100$  nm, and is similar to that reported by Anderson's group for their quinoidal triply linked porphyrin dimer, which had a HOMO-LUMO gap of 1.00 V.<sup>[27]</sup> The fused dizinc diporphyrin studied by Diederich and co-workers showed a HOMO-LUMO gap of 1.10 V in CH<sub>2</sub>Cl<sub>2</sub>,<sup>[26]</sup> whereas tetraprotonated  $\beta$ - $\beta$ -directly linked N-confused porphyrin dimers exhibited electrochemical HOMO-LUMO gaps of  $\leq 1.11$  V.<sup>[28]</sup>

## Conclusion

Monomeric zinc(II) *meso*- $\eta^1$ -organoplatinum porphyrins were readily dimerized by silver(I) oxidative coupling to give the *meso-meso* singly linked dimer **5** in high yields. Oxidative double ring closure was also facile and provided easy access to triply linked porphyrin dimers with organometallic termini. Electrochemical measurements of the former dimer demonstrated that the organometallic fragment was a good electron donor. This trend was maintained after fusion and planarization to generate a very easily oxidizable triply linked bis-zinc(II) dimer **8**, with a narrow electrochemical HOMO-LUMO gap of about 0.96 V, and its lowest-energy electronic absorption band near  $\lambda = 1100$  nm. Although the triply linked dimers proved to be too sensitive for the growth of high-quality single crystals, the crystal structure of the singly linked bis-nickel(II) analogue **10** confirmed the attachment of terminal *trans*-[Pt(PPh<sub>3</sub>)<sub>2</sub>Br] fragments. Incorporation of these organometallic porphyrins into supramolecular arrangements and their attachment to surfaces and electrodes may be rewarding in the future.

## Experimental Section

### General Procedures

Syntheses that involved zero-valent metal precursors were carried out in an atmosphere of high-purity argon by using conventional Schlenk techniques. Porphyrin starting materials, 5,15-diphenylporphyrin<sup>[29]</sup> and [Pt-(dba)<sub>2</sub>]<sub>2</sub>,<sup>[30]</sup> were prepared by methods reported in the literature. All other reagents and ligands were used as received from Sigma-Aldrich. Toluene was AR grade, stored over sodium wire, and degassed by purging with argon at about 90 °C. All other solvents were AR grade, and dichloromethane and chloroform were stored over anhydrous sodium carbonate. Analytical TLC was performed by using Merck silica gel 60 F<sub>254</sub> plates and column chromatography was performed by using Merck silica gel (230-400 mesh; Brisbane) and Wakogel C-300 or C-400 (Kyoto). NMR spectra were recorded in Brisbane on Bruker Avance 400 MHz or Varian Unity 300 MHz instruments in CDCl<sub>3</sub>, with CHCl<sub>3</sub> as the internal reference at  $\delta = 7.26$  ppm for <sup>1</sup>H spectra, and external 85% H<sub>3</sub>PO<sub>4</sub> as the reference for proton-decoupled <sup>31</sup>P spectra. <sup>1</sup>H NMR spectra were recorded in Kyoto on a JEOL ECA-600 spectrometer (operating at 600.17 MHz for <sup>1</sup>H and 242.95 MHz for <sup>31</sup>P). UV/Vis spectra were recorded on a Cary 3 spectrometer (Brisbane) and a Shimadzu UV-3600PC spectrometer (Kyoto) in dichloromethane. Near-IR measurements were carried out on a Nicolet Nexus FTIR instrument equipped with a quartz halogen lamp, quartz beam splitter, and an InGaAs detector operating at room temperature.

X-ray data for compound **10** were collected at -180 °C with a Rigaku RAXIS-RAPID diffractometer by using graphite monochromated Cu<sub>K $\alpha$</sub>  radiation ( $\lambda = 1.54187$  Å). The structures were solved by direct methods

(SHELXS-97).<sup>[31]</sup> ESI mass spectra were recorded on a Bruker BioApex 47e FTMS instrument fitted with an Analytica electrospray source. The samples were dissolved in dichloromethane and diluted with either 1:1 dichloromethane/methanol or methanol and solutions were introduced into the source by direct infusion (syringe pump) at 60  $\mu\text{L h}^{-1}$ , with a capillary voltage of 80 V. The instrument was calibrated by using internal NaI clusters. Positive ion FAB mass spectra were recorded on a Kratos Concept instrument at the Central Science Laboratory, University of Tasmania. Samples were dissolved in dichloromethane and dispersed in a 4-nitrobenzyl alcohol matrix. In the data below, masses given are for the strongest observed peak in the molecular ion cluster. In all compounds, this  $m/z$  value agreed with the predicted molecular mass, although in most cases it represented a mixture of  $[M]$  and  $[M+1]$  peaks. The accurate-mass ESI-TOF mass spectrum of **10** was recorded on a Bruker microTOF model in positive mode in acetonitrile. Elemental analyses were carried out by the Microanalytical Service, The University of Queensland. For electrochemical measurements, a standard three-electrode configuration was used, with a Pt button working electrode and a Pt wire counter electrode. The reference electrode comprised a silver wire coated with silver chloride separated from the working solution by two fritted jackets. The internal chamber containing the wire was filled with 0.05 M  $\text{Bu}_4\text{NCl}/0.45$  M  $\text{Bu}_4\text{NPF}_6$ , and the external chamber contacting the working solution was filled with 0.5 M  $\text{Bu}_4\text{PF}_6$ , all solutions were prepared in  $\text{CH}_2\text{Cl}_2$ . The working solution was pre-purged and subsequently protected with ultra-high purity  $\text{N}_2$ . The voltammetry measurements were carried out in  $\text{CH}_2\text{Cl}_2$  (freshly distilled from  $\text{CaH}_2$  under argon) containing 0.5 M  $\text{Bu}_4\text{NPF}_6$ , using an EG&G Princeton Applied Research Model 272A Potentiostat linked to a PC interface and controlled by PowerSuite software. Electrode potentials are reported by using ferrocene as an internal standard ( $E^0 = 0.00$  V).

*trans-Bromido[10,20-diphenylporphyrinato-5-yl]bis(triphenylphosphine)platinum(II) 3*

Toluene (200 mL) was added to a Schlenk flask and degassed by bubbling argon through the solution at 90°C. Bromoporphyrin **2** (200 mg, 0.37 mmol) was added and stirred for 5 min.  $[\text{Pt}(\text{dba})_2]$  (290 mg, 0.44 mmol) and triphenylphosphine (346 mg, 1.32 mmol) were added and the solution was stirred at 90°C. TLC analysis of the reaction mixture (50%  $\text{CHCl}_3/49\%$  hexane/1%  $\text{Et}_3\text{N}$ ) clearly showed disappearance of the starting material after about 30 min and that the initially formed *cis* isomer was slowly being converted into the *trans* isomer. After about 6 h, isomerization was considered complete and the reaction mixture was cooled to room temperature and the solvent removed under reduced pressure. The residue (now air stable) was purified on a silica gel column eluting with 50%  $\text{CHCl}_3/49\%$  hexane/1%  $\text{Et}_3\text{N}$  and the major purple fraction was collected and the solvent removed in vacuo. The residue was recrystallized from  $\text{CHCl}_3/\text{pentane}$  to give **3** as dark purple crystals (431 mg, 94%). The  $^1\text{H}$  and  $^{31}\text{P}$  NMR spectroscopic data for this compound agreed with those of an authentic sample prepared previously with  $[\text{Pt}(\text{PPh}_3)_3]$ .<sup>[7]</sup>

*trans-Bromo[10,20-diphenylporphyrinatozinc(II)-5-yl]bis(triphenylphosphine)platinum(II) 4*

Free-base **3** (200 mg, 0.16 mmol) was dissolved in  $\text{CHCl}_3$  (100 mL) and  $\text{Zn}(\text{OAc})_2$  (200 mg, 1.1 mmol) was added as a concentrated solution in methanol. The solution was heated at reflux for 1 h and cooled to room temperature. This solution was concentrated to approximately 50 mL and applied to a short silica-gel chromatography column. The column was eluted with  $\text{CHCl}_3$  and the major purple/green band collected. The solvent was removed under reduced pressure and the residue recrystallized from  $\text{CHCl}_3/\text{pentane}$  to give **4** as metallic purple crystals (208 mg, 97%). The  $^1\text{H}$  and  $^{31}\text{P}$  NMR spectroscopic data for this compound agreed with those of an authentic sample.<sup>[7b]</sup>

*meso,meso-Bis[trans-bromido[10,20-diphenylporphyrinatozinc(II)-5-yl]bis(triphenylphosphine)platinum(II)] 5*

$[\text{AgPF}_6]$  (95 mg, 0.375 mmol) was added as a solution in acetonitrile to a solution of monomer **4** (100 mg, 0.075 mmol) in  $\text{CHCl}_3$  (50 mL). The

reaction vessel was protected from light and the mixture was stirred for 1 h. LiBr (100 mg, 1.15 mmol) was added to the reaction mixture and the solution was heated at reflux for 30 min. A solution of  $\text{Zn}(\text{OAc})_2$  (100 mg, 0.55 mmol) in methanol was added and the solution further heated at reflux for 1 h. The reaction mixture was cooled to room temperature and the solvent removed under reduced pressure. The dark green residue was purified by column chromatography (66%  $\text{CHCl}_3/\text{hexane}$ ) and the major band collected. The solution was evaporated to dryness and the residue recrystallized from  $\text{CHCl}_3/\text{pentane}$  to give dimer **5** (91 mg, 92%).  $^1\text{H}$  NMR:  $\delta = 6.40\text{--}6.60$  (m, 36H;  $\text{PPh}_3$ ), 7.30–7.40 (m, 12H;  $\text{PPh}_3$ ), 7.55–7.65 (m, 12H; *m,p*-H on 10,20-phenyl), 8.05–8.15 (m, 8H; *o*-H on 10,20-phenyl), 7.98, 8.47, 8.50, 9.30 ppm (each d,  $^3J = 4.7$  Hz, 4H;  $\beta$ -H);  $^{31}\text{P}$  NMR:  $\delta = 23.5$  ppm (s,  $^1J(\text{P,Pt}) = 2990$  Hz); UV/Vis:  $\lambda_{\text{max}}(\epsilon/10^3) = 437$  (210), 470 (221), 571 (42.0), 610 nm ( $17.0 \text{ mol}^{-1} \text{ m}^3 \text{ cm}^{-1}$ ); elemental analysis calcd (%) for  $\text{C}_{136}\text{H}_{96}\text{Br}_2\text{N}_8\text{P}_4\text{Pt}_2\text{Zn}_2$ : C 61.71, H 3.66, N 4.23; found: C 61.68, H 3.52, N 4.16.

*meso-meso, $\beta$ - $\beta$ , $\beta$ -Bis[trans-bromido[10,20-diphenylporphyrinatozinc(II)-5-yl]bis(triphenylphosphine)platinum(II)] 8*

Directly *meso-meso*-linked dimer **5** (50 mg, 0.019 mmol) was dissolved in dry toluene (25 mL) under an argon atmosphere.  $\text{Sc}(\text{OTf})_3$  (47 mg, 0.095 mmol) and DDO (22 mg, 0.095 mmol) were added and the mixture was heated at reflux for 1 h. The mixture was cooled to room temperature and the solvent removed under reduced pressure. The residue was dissolved in minimum ethyl acetate and loaded onto a short silica-gel column and eluted with ethyl acetate. The blue/green fraction was collected, the solvent removed, and the residue recrystallized from  $\text{CHCl}_3/\text{cyclohexane}$ . Product **5** was collected as a very dark blue/green solid (34 mg, 68%).  $^1\text{H}$  NMR:  $\delta = 6.80\text{--}6.90$  (m, 36H;  $\text{PPh}_3$ ), 7.19 (s, 4H; 2,2',8,8'- $\beta$ -H), 7.26 (d,  $^3J = 4.4$  Hz, 4H; 12,12',18,18'- $\beta$ -H), 7.30–7.50 (m, 24H;  $\text{PPh}_3$ ), 7.50–7.60 (m, 12H; *m,p*-H on 10,20-phenyl), 7.70–7.80 (m, 8H; *o*-H on 10,20-phenyl), 8.72 ppm (d,  $^3J = 4.4$  Hz, 4H; 13,13',17,17'- $\beta$ -H);  $^{31}\text{P}$  NMR:  $\delta = 22.7$  ppm (s,  $^1J(\text{P,Pt}) = 3016$  Hz); UV/Vis:  $\lambda_{\text{max}}(\epsilon/10^3) = 426$  (59.7), 489 (40.5), 608 (88.5), 670 sh (25.2), 936 sh (11.9), 1066 nm ( $33.4 \text{ mol}^{-1} \text{ m}^3 \text{ cm}^{-1}$ ); ESI MS:  $m/z$  calcd for  $\text{C}_{136}\text{H}_{96}\text{Br}_2\text{N}_8\text{P}_4\text{Pt}_2\text{Zn}_2(+1)$ : 2643.27; found: 2643.26; elemental analysis calcd (%) for  $\text{C}_{136}\text{H}_{96}\text{Br}_2\text{N}_8\text{P}_4\text{Pt}_2\text{Zn}_2 \cdot 2\text{CH}_2\text{Cl}_2$ : C 58.93, H 3.44, N 3.98; found: C 58.79, H 3.28, N 3.91.

*meso-meso, $\beta$ - $\beta$ , $\beta$ -Bis[trans-bromido[10,20-diphenylporphyrinato-5-yl]bis(triphenylphosphine)platinum(II)] 9*

HCl (500  $\mu\text{L}$  of a 2 M solution in methanol) was added to a stirred solution of metallated **8** (3 mg, 0.0014 mmol) in  $\text{CHCl}_3$ . The solution immediately turned purple and was neutralized with  $\text{Et}_3\text{N}$  (1 mL), after which it changed back to a deep blue/green color. The  $\text{CHCl}_3$  layer was washed twice with water and dried over anhydrous  $\text{MgSO}_4$ . The solvent was removed under reduced pressure and dried thoroughly under high vacuum at 50°C for 2 h. Free-base **9** was formed quantitatively and was pure according to  $^1\text{H}$  and  $^{31}\text{P}$  NMR spectroscopy.  $^1\text{H}$  NMR:  $\delta = 6.80\text{--}6.90$  (m, 36H;  $\text{PPh}_3$ ), 7.0 (s, 4H; 2,2',8,8'- $\beta$ -H), 7.19 (d,  $^3J = 4.0$  Hz, 4H; 12,12',18,18'- $\beta$ -H), 7.40–7.50 (m, 24H;  $\text{PPh}_3$ ), 7.50–7.60 (m, 12H; *m,p*-H on 10,20-phenyl), 7.60–7.70 (m, 8H; *o*-H on 10,20-phenyl), 8.74 ppm (d,  $^3J = 4.0$  Hz, 4H; 13,13',17,17'- $\beta$ -H);  $^{31}\text{P}$  NMR:  $\delta = 23.3$  ppm (s,  $^1J(\text{P,Pt}) = 2996$  Hz); UV/Vis:  $\lambda_{\text{max}}$  (rel. int.) 422 (4.9), 488 (3.5), 604 (6.0), 934 sh (1.0), 1055 nm (2.1).

*meso-meso-Bis[trans-bromido[10,20-diphenylporphyrinato-nickel(II)-5-yl]bis(triphenylphosphine)platinum(II)] 10*

Directly *meso-meso*-linked dimer **5** (10 mg, 3.8  $\mu\text{mol}$ ) was dissolved in  $\text{CHCl}_3$  (5 mL) and aqueous HCl (100  $\mu\text{L}$  of a 3 M solution) was added to the reaction solution and stirred for 2.5 h at room temperature. The reaction mixture was washed with aqueous  $\text{Na}_2\text{CO}_3$  and the products were extracted with  $\text{CH}_2\text{Cl}_2$ . The organic extract was dried over anhydrous  $\text{Na}_2\text{SO}_4$ , and the solvent was evaporated under reduced pressure. The residue was dissolved in toluene (5 mL) and nickel acetylacetonate (29 mg, 30 equiv) was added and the solution was heated at reflux for 3 h. The reaction mixture was cooled to room temperature and the solvent removed under reduced pressure. The residue was purified by column chromatog-

raphy (50% CH<sub>2</sub>Cl<sub>2</sub>/hexane) and the major band collected. The solution was evaporated to dryness and the residue recrystallized from CH<sub>2</sub>Cl<sub>2</sub>/hexane to give complex **10** (7.0 mg, 70%). <sup>1</sup>H NMR: δ = 6.6–6.8 (m, 36H; PPh<sub>3</sub>), 7.32 (m, 24H; PPh<sub>3</sub>), 7.45–7.55 (m, 12H; *m,p*-H on 10,20-phenyl), 7.84 (m, 8H; *o*-H on 10,20-phenyl), 7.93, 8.17, 8.27, 9.44 ppm (each d, <sup>3</sup>J = 4.7 Hz, 4H; β-H); <sup>31</sup>P NMR: δ = 22.78 ppm (s, <sup>1</sup>J(P,Pt) = 2927 Hz); UV/Vis: λ<sub>max</sub>(ε/10<sup>3</sup>) = 436 (153), 464 (241), 552 nm (51.4 mol<sup>-1</sup>m<sup>3</sup>cm<sup>-1</sup>); ESI-HRMS: *m/z* calcd for C<sub>136</sub>H<sub>96</sub>N<sub>8</sub>P<sub>4</sub>Br<sub>2</sub>Ni<sub>2</sub>Pt<sub>2</sub>[M]<sup>+</sup>: 2633.3058; found 2633.3045.

#### Crystal Data for **10**

C<sub>136</sub>H<sub>96</sub>Br<sub>2</sub>N<sub>8</sub>Ni<sub>2</sub>P<sub>4</sub>Pt<sub>2</sub>·2.5(C<sub>5</sub>H<sub>12</sub>); *M*<sub>r</sub> = 2813.87; triclinic; space group *P* $\bar{1}$  (no. 2); *a* = 13.8776(3), *b* = 19.9966(4), *c* = 24.1466(4) Å; α = 101.1999(10), β = 93.5439(10), γ = 107.1007(11)°; *V* = 6231.8(2) Å<sup>3</sup>; *Z* = 2; ρ<sub>calcd</sub> = 1.500 g cm<sup>-3</sup>; *T* = 93 K; *R*<sub>1</sub> = 0.1306 [*I* > 2σ(*I*)]; *R*<sub>w</sub> = 0.3897 (all data); GOF = 1.025. Crystals were grown from CH<sub>2</sub>Cl<sub>2</sub>/*n*-pentane. CCDC 936169 contains the supplementary crystallographic data for the complex **10**. These data can be obtained free of charge from the Cambridge Crystallographic Data Centre via www.ccdc.cam.ac.uk/data\_request/cif.

### Acknowledgements

R.D.H. thanks the Faculty of Science, Queensland University of Technology, for a Post-Graduate Scholarship, and Dr. Llew Rintoul for the near-IR measurements. T.Y. and H.M. thank the JSPS for Fellowships for Young Scientists.

- [1] a) P. J. Brothers, *Adv. Organomet. Chem.* **2000**, *46*, 223–321; b) R. Guilard, A. Tabard, E. van Caemelbecke, K. M. Kadish in *The Porphyrin Handbook, Vol. 3* (Eds.: K. M. Kadish, K. M. Smith, R. Guilard), Academic Press, San Diego, **2000**, pp. 295–346.
- [2] For a selection of recent references to N-confused (inverted), carba-porphyrins, and azuliporphyrins with organometallic bonds, see: a) M. Pawlicki, L. Latos-Grażyński in *Handbook of Porphyrin Science, Vol. 2* (Eds.: K. M. Kadish, K. M. Smith, R. Guilard), World Scientific Publishing, Singapore, **2010**, pp. 103–192; b) N. Grzegorzec, L. Latos-Grażyński, L. Sztterenber, *Org. Biomol. Chem.* **2012**, *10*, 8064–8075; c) M. Toganoh, H. Furuta in *Handbook of Porphyrin Science, Vol. 2* (Eds.: K. M. Kadish, K. M. Smith, R. Guilard), World Scientific Publishing, Singapore, **2010**, pp. 295–367; d) T. D. Lash in *Handbook of Porphyrin Science, Vol. 16* (Eds.: K. M. Kadish, K. M. Smith, R. Guilard), World Scientific Publishing, Singapore, **2010**, pp. 1–329; e) T. D. Lash, K. Pokharel, M. Zeller, G. M. Ference, *Chem. Commun.* **2012**, *48*, 11793–11795; f) T. D. Lash, *Org. Lett.* **2011**, *13*, 4632–4635; g) P. Jain, G. M. Ference, T. D. Lash, *J. Org. Chem.* **2010**, *75*, 6563–6573; h) P. J. Chmielewski, *Inorg. Chem.* **2009**, *48*, 432–445; i) P. J. Chmielewski, L. Latos-Grażyński, *Coord. Chem. Rev.* **2005**, *249*, 2510–2533; j) T. D. Lash, D. A. Colby, L. F. Szczepura, *Inorg. Chem.* **2004**, *43*, 5258–5267; k) T. D. Lash, D. A. Colby, S. R. Graham, G. M. Ference, L. F. Szczepura, *Inorg. Chem.* **2003**, *42*, 7326–7338; l) M. Pawlicki, I. Kańska, L. Latos-Grażyński, *Inorg. Chem.* **2007**, *46*, 6575–6584.
- [3] See, for example: a) K. Naoda, H. Mori, A. Osuka, *Chem. Lett.* **2013**, *42*, 22–24; b) T. Tanaka, N. Aratani, A. Osuka, *Chem. Asian J.* **2012**, *7*, 889–893; c) K. Naoda, H. Mori, N. Aratani, B. S. Lee, D. Kim, A. Osuka, *Angew. Chem.* **2012**, *124*, 9994–9997; *Angew. Chem. Int. Ed.* **2012**, *51*, 9856–9859; d) T. Tanaka, A. Osuka, *Chem. Eur. J.* **2012**, *18*, 7036–7040; e) T. Yoneda, S. Saito, H. Yorimitsu, A. Osuka, *Angew. Chem.* **2011**, *123*, 3537–3540; *Angew. Chem. Int. Ed.* **2011**, *50*, 3475–3478; f) T. Tanaka, T. Sugita, S. Saito, A. Osuka, *Angew. Chem.* **2010**, *122*, 6769–6771; *Angew. Chem. Int. Ed.* **2010**, *49*, 6619–6621.
- [4] a) S. W. Rhee, Y. H. Na, Y. Do, J. Kim, *Inorg. Chim. Acta* **2000**, *309*, 49–56; b) S. W. Rhee, B. B. Park, Y. Do, J. Kim, *Polyhedron* **2000**, *19*, 1961–1966; c) A. K. Burrell, W. M. Campbell, G. B. Jameson, D. L. Officer, P. D. W. Boyd, Z. Zhao, P. A. Cocks, K. C. Gordon, *Chem. Commun.* **1999**, 637–638; d) O. Shoji, S. Okada, A. Satake, Y. Kobuke, *J. Am. Chem. Soc.* **2005**, *127*, 2201–2210; e) H. J. H. Wang, L. Jaquinod, D. J. Nurco, M. G. H. Vicente, K. M. Smith, *Chem. Commun.* **2001**, 2646–2647; f) K. K. Dailey, T. B. Rauchfuss, *Polyhedron* **1997**, *16*, 3129–3138; g) K. K. Dailey, G. P. A. Yap, A. L. Rheingold, T. B. Rauchfuss, *Angew. Chem.* **1996**, *108*, 1985–1987; *Angew. Chem. Int. Ed. Engl.* **1996**, *35*, 1833–1835; h) S. Yamaguchi, H. Shinokubo, A. Osuka, *J. Am. Chem. Soc.* **2010**, *132*, 9992–9993.
- [5] a) S. Richeter, C. Jeandon, J.-P. Gisselbrecht, R. Ruppert in *Handbook of Porphyrin Science, Vol. 3* (Eds.: K. M. Kadish, K. M. Smith, R. Guilard), World Scientific Publishing, Singapore, **2010**, pp. 429–483; b) F. Atefi, D. P. Arnold, *J. Porphyrins Phthalocyanines* **2008**, *12*, 801–831; c) B. M. J. M. Suijkerbuijk, R. J. M. Klein Gebbink, *Angew. Chem.* **2008**, *120*, 7506–7532; *Angew. Chem. Int. Ed.* **2008**, *47*, 7396–7421.
- [6] D. P. Arnold, Y. Sakata, K.-i. Sugiura, E. I. Worthington, *Chem. Commun.* **1998**, 2331–2332.
- [7] a) D. P. Arnold, P. C. Healy, M. J. Hodgson, M. L. Williams, *J. Organomet. Chem.* **2000**, *607*, 41–50; b) M. J. Hodgson, P. C. Healy, M. L. Williams, D. P. Arnold, *J. Chem. Soc. Dalton Trans.* **2002**, 4497–4504; c) R. D. Hartnell, A. J. Edwards, D. P. Arnold, *J. Porphyrins Phthalocyanines* **2002**, *6*, 695–707.
- [8] M. J. Hodgson, V. V. Borovkov, Y. Inoue, D. P. Arnold, *J. Organomet. Chem.* **2006**, *691*, 2162–2170.
- [9] a) R. D. Hartnell, D. P. Arnold, *Eur. J. Inorg. Chem.* **2004**, 1262–1269; b) R. D. Hartnell, D. P. Arnold, *Organometallics* **2004**, *23*, 391–399.
- [10] a) S. Anabuki, H. Shinokubo, N. Aratani, A. Osuka, *Angew. Chem.* **2012**, *124*, 3228–3231; *Angew. Chem. Int. Ed.* **2012**, *51*, 3174–3177; b) K. Yoshida, T. Nakashima, S. Yamaguchi, A. Osuka, H. Shinokubo, *Dalton Trans.* **2011**, *40*, 8773–8775; c) J. Yamamoto, T. Shimizu, S. Yamaguchi, N. Aratani, H. Shinokubo, A. Osuka, *J. Porphyrins Phthalocyanines* **2011**, *15*, 534–538; d) J. Song, N. Aratani, J. H. Heo, D. Kim, H. Shinokubo, A. Osuka, *J. Am. Chem. Soc.* **2010**, *132*, 11868–11869; e) K. Yoshida, S. Yamaguchi, A. Osuka, H. Shinokubo, *Organometallics* **2010**, *29*, 3997–4000; f) S. Yamaguchi, H. Shinokubo, A. Osuka, *Inorg. Chem.* **2009**, *48*, 795–797; g) S. Yamaguchi, T. Katoh, H. Shinokubo, A. Osuka, *J. Am. Chem. Soc.* **2008**, *130*, 14440–14441; h) S. Yamaguchi, T. Katoh, H. Shinokubo, A. Osuka, *J. Am. Chem. Soc.* **2007**, *129*, 6392–6393.
- [11] a) Y. Matano, K. Matsumoto, H. Hayashi, Y. Nakao, T. Kumpulainen, V. Chukharev, N. V. Tkachenko, H. Lemmetyinen, S. Shimizu, N. Kobayashi, D. Sakamaki, A. Ito, K. Tanaka, H. Imahori, *J. Am. Chem. Soc.* **2012**, *134*, 1825–1839; b) Y. Matano, K. Matsumoto, Y. Nakao, H. Uno, S. Sakaki, H. Imahori, *J. Am. Chem. Soc.* **2008**, *130*, 4588–4589.
- [12] a) H. Furuta, N. Kubo, H. Maeda, T. Ishizuka, A. Osuka, H. Nanami, T. Ogawa, *Inorg. Chem.* **2000**, *39*, 5424–5425; b) H. Furuta, K. Youfu, H. Maeda, A. Osuka, *Angew. Chem.* **2003**, *115*, 2236–2238; *Angew. Chem. Int. Ed.* **2003**, *42*, 2186–2188; c) P. J. Chmielewski, I. Schmidt, *Inorg. Chem.* **2004**, *43*, 1885–1894; d) P. J. Chmielewski, B. Durlej, M. Siczek, L. Sztterenber, *Angew. Chem.* **2009**, *121*, 8892–8895; *Angew. Chem. Int. Ed.* **2009**, *48*, 8736–8739.
- [13] For a selection of recent references for palladium-catalyzed porphyrin reactions, see: a) K. B. Fields, J. V. Ruppel, N. L. Snyder, X. P. Zhang in *Handbook of Porphyrin Science, Vol. 3* (Eds.: K. M. Kadish, K. M. Smith, R. Guilard), World Scientific Publishing, Singapore, **2010**, pp. 367–427; b) N. N. Sergeeva, M. O. Senge, A. Ryan in *Handbook of Porphyrin Science, Vol. 3* (Eds.: K. M. Kadish, K. M. Smith, R. Guilard), World Scientific Publishing, Singapore, **2010**, pp. 325–365; c) N. Sugita, S. Hayashi, F. Hino, T. Takanami, *J. Org. Chem.* **2012**, *77*, 10488–10497; d) L. J. Esdaile, J. C. McMurtrie, P. Turner, D. P. Arnold, *Tetrahedron Lett.* **2005**, *46*, 6931–6935; e) L. J. Esdaile, M. O. Senge, D. P. Arnold, *Chem. Commun.* **2006**, 4192–4194; f) F. Atefi, J. C. McMurtrie, P. Turner, M. Duriska, D. P. Arnold, *Inorg. Chem.* **2006**, *45*, 6479–6489; g) O. B. Locos, B. Bašić, J. C. McMurtrie, P. Jensen, D. P. Arnold, *Chem. Eur. J.* **2012**, *18*, 5574–5588; h) K. Ladomenou, T. Lazarides, M. K. Panda, G. Chara-

- lambidis, D. Daphnomili, A. G. Coutsolelos, *Inorg. Chem.* **2012**, *51*, 10548–10556; i) M. Y. Jiang, J.-Y. Shin, B. O. Patrick, D. Dolphin, *J. Chem. Soc. Dalton Trans.* **2008**, *19*, 2598–2602.
- [14] a) N. Aratani, A. Osuka, *Bull. Chem. Soc. Jpn.* **2001**, *74*, 1361–1379; b) N. Aratani, A. Tsuda, A. Osuka, *Synlett* **2001**, 1663–1674; c) A. Nakano, A. Osuka, I. Yamazaki, T. Yamazaki, Y. Nishimura, *Angew. Chem.* **1998**, *110*, 3172–3176; *Angew. Chem. Int. Ed.* **1998**, *37*, 3023–3027.
- [15] A. Osuka, H. Shimidzu, *Angew. Chem.* **1997**, *109*, 93–95; *Angew. Chem. Int. Ed. Engl.* **1997**, *36*, 135–137.
- [16] A. Tsuda, H. Furuta, A. Osuka, *J. Am. Chem. Soc.* **2001**, *123*, 10304–10321.
- [17] A. Tsuda, A. Osuka, *Science* **2001**, *293*, 79–82.
- [18] N. Yoshida, T. Ishizuka, A. Osuka, D. H. Jeong, H. S. Cho, D. Kim, Y. Matsuzaki, A. Nogami, K. Tanaka, *Chem. Eur. J.* **2003**, *9*, 58–75.
- [19] a) M. O. Senge, M. Pinteá, A. A. Ryan, *Z. Naturforsch. B* **2011**, *66*, 0553–0558; b) R. G. Houry, L. Jaquinod, K. M. Smith, *Chem. Commun.* **1997**, 1057–1058.
- [20] a) N. Aratani, A. Osuka, *Chem. Commun.* **2008**, 4067–4069; b) N. Aratani, A. Takagi, Y. Yanagawa, T. Matsumoto, T. Kawai, Z. S. Yoon, D. Kim, A. Osuka, *Chem. Eur. J.* **2005**, *11*, 3389–3404.
- [21] J. Song, N. Aratani, P. Kim, D. Kim, H. Shinokubo, A. Osuka, *Angew. Chem.* **2010**, *122*, 3699–3702; *Angew. Chem. Int. Ed.* **2010**, *49*, 3617–3620.
- [22] M. O. Senge, *Chem. Commun.* **2006**, 243–256.
- [23] a) B. Bašić, J. C. McMurtrie, D. P. Arnold, *J. Porphyrins Phthalocyanines* **2010**, *14*, 481–493; b) L. J. Esdaile, P. Jensen, J. C. McMurtrie, D. P. Arnold, *Angew. Chem.* **2007**, *119*, 2136–2139; *Angew. Chem. Int. Ed.* **2007**, *46*, 2090–2093.
- [24] M. J. Hodgson, M.App.Sci. Thesis, Queensland University of Technology (Australia), **2005**.
- [25] a) D. P. Arnold, G. A. Heath, *J. Am. Chem. Soc.* **1993**, *115*, 12197–12198; b) D. P. Arnold, G. A. Heath, D. A. James, *J. Porphyrins Phthalocyanines* **1999**, *3*, 5–31; c) G. J. Wilson, D. P. Arnold, *J. Phys. Chem. A* **2005**, *109*, 6104–6113.
- [26] D. Bonifazi, M. Scholl, F. Song, L. Echegoyen, G. Accorsi, N. Armaroli, F. Diederich, *Angew. Chem.* **2003**, *115*, 5116–5120; *Angew. Chem. Int. Ed.* **2003**, *42*, 4966–4970.
- [27] I. M. Blake, A. Krivokapic, M. Katterle, H. L. Anderson, *Chem. Commun.* **2002**, 1662–1663.
- [28] P. J. Chmielewski, M. Siczek, L. Sztterenber, *Inorg. Chem.* **2011**, *50*, 6719–6736.
- [29] a) S. G. DiMugno, V. S. Y. Lin, M. J. Therien, *J. Org. Chem.* **1993**, *58*, 5983–5993; b) J. S. Manka, D. S. Lawrence, *Tetrahedron Lett.* **1989**, *30*, 6989–6992.
- [30] W. J. Cherwinski, B. F. G. Johnson, J. Lewis, *J. Chem. Soc. Dalton Trans.* **1974**, 1405–1409.
- [31] G. Sheldrick, T. Schneider, *Methods Enzymol.* **1997**, *277*, 319.

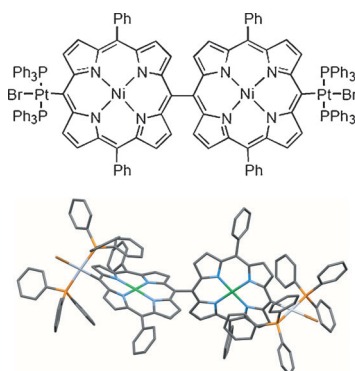
Received: May 6, 2013

Revised: May 27, 2013

Published online: ■ ■ ■, 0000

# FULL PAPER

**Closing the gap:** *meso-meso*-Directly linked and *meso-meso*, $\beta$ - $\beta$ , $\beta$ - $\beta$ -triply linked diporphyrins terminated by *trans*-[Pt(PPh<sub>3</sub>)<sub>2</sub>Br] units are described (see picture). The organometallic substituents raise the HOMO levels such that the dimers are very easily oxidized, and the fused Zn<sub>2</sub> dimer has a voltammetric HOMO-LUMO gap of only 0.96 eV.



## Porphyrids

Regan D. Hartnell, Tomoki Yoneda,  
Hirotaka Mori, Atsuhiko Osuka,\*

Dennis P. Arnold\* ———— ■■■■-■■■■

**The Marriage of Peripherally Metal-  
lated and Directly Linked Porphyrins:  
Bromidobis(phosphine)platinum(II) as  
a Cation-Stabilizing Substituent on  
Directly Linked and Fused Triply  
Linked Diporphyrins**

